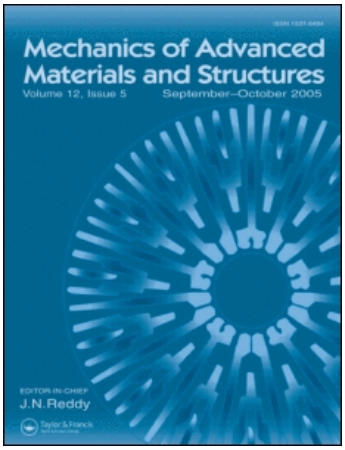

Mechanics of Advanced Materials and Structures
Publication details, including instructions for authors and subscription information: http://www-intra.informaworld.com/smpp/title~content=t713773278

Three-Dimensional Modeling of Functionally Graded Multiferroic Composites

Ruifeng Wang[a]; Ernian Pan[a]
[a] Computer Modeling and Simulation Group, University of Akron, Akron, Ohio, USA

Online publication date: 24 January 2011

To cite this Article Wang, Ruifeng and Pan, Ernian(2011) 'Three-Dimensional Modeling of Functionally Graded Multiferroic Composites', Mechanics of Advanced Materials and Structures, 18: 1, 68 — 76
To link to this Article: DOI: 10.1080/15376494.2010.519227
URL: http://dx.doi.org/10.1080/15376494.2010.519227

Mechanics of Advanced Materials and Structures, 18:68–76, 2011

ISSN: 1537-6494 print / 1537-6532 online
DOI: 10.1080/15376494.2010.519227

Taylor & Francis
Taylor & Francis Group

Three-Dimensional Modeling of Functionally Graded Multiferroic Composites

Ruifeng Wang and Ernian Pan
Computer Modeling and Simulation Group, University of Akron, Akron, Ohio USA

A three-dimensional (3D) finite-element-method (FEM) formulation is developed to investigate the response of functionally graded material (FGM) multiferroic composites under different types of loads. Numerical examples are carried out for the three-layered piezoelectric (PE)/piezomagnetic (PM) composite with its top and bottom layers being FGMs and the middle layer homogenous PE material. For the FGM layer, two cases of material grading along the thickness direction of the composite are considered: one is the PM material with the properties varying as an exponential function (E-FGM) and the other is the PE/PM composite material with the volume ratios varying as a power-law function (P-FGM). The effect of different material grading functions on the mechanical, electric and magnetic responses is clearly showed by both E-FGM and P-FGM grading cases, which could be useful to the future design of FGM multiferroic devices.

Keywords FEM, multiferroic, piezoelectric, piezomagnetic, magnetoelectric, FGM, composite

1. INTRODUCTION

Multiferroic structures composed of piezoelectric (PE) and piezomagnetic (PM) materials have the magneto-electro-elastic (MEE) coupling property, with ability to convert energy from one form (among magnetic, electric, and mechanical energies) to the other. Research [1–7] has been conducted to investigate the magnetoelectric (ME) effect in the past two decades. As for the full-field study, the analytical solution based on the Stroh formulism and propagator matrix method has been proposed to study the static and vibration responses of the MEE plates under certain simple lateral boundary conditions [8, 9]. Similar methods [10] were also applied to the cylindrical bending problem of MEE laminated structures with simply supported edges. As for the numerical modeling, the semi-analytical layer-wise finite element methods (FEM) were proposed for the MEEplates in [11, 12].

Received 18 June 2009; accepted 19 September 2009.
Address correspondence to Ernian Pan, Computer Modeling and Simulation Group, College of Engineering, University of Akron, Akron, OH 44325-3905, USA. E-mail: pan2@uakron.edu

Functionally graded materials (FGMs) can be fabricated by continuously changing the volume fraction of the material, resulting in gradual changes in material properties. The concept of FGMs was first proposed in 1984 by material scientists when preparing thermal barrier materials [13, 14]. Since then FGMs have been applied to various fields, for instance, used as an interfacial zone material to improve the anti-cracking strength [15, 16], applied to improve the electrochemical performance of fuel cells [17, 18], and applied to biomechanics [19–21]. Some analytical and numerical discussions for single-phase FGM structure have been conducted: an exact solution was provided for layered elastic FGM structure under simply-supported boundary condition [22]; an analytical solution was obtained for a piezoelectric functionally graded layered half space under uniform circular surface loadings [23]; a two-dimensional (2D) FEM for simulating purely elastic FGM structures and for determining the stress intensity factors were discussed in [24, 25]. By extending the multiferroic problem to FGMs, Pan and Han [26] provided an exact static solution for the exponential functionally graded (E-FGM) layered magneto-electro-elastic composites. The discrete layer model was employed to investigate the free vibration properties for FGM magneto-electro-elastic composites in [27].

In this article, we present a 3D FEM model for multiferroic FGM composites. In our 3D FEM program for layered FGM multiferroic structures, the continuously varying material properties in the PE or PM layer is taken into account and the material gradient can be defined with different functions and along different directions. As numerical examples, the exponential (E-FGM) and power-law (P-FGM) functions are used to define the variation of the material properties along the grading direction. In the study of E-FGM case, a three-layered MEE plate with fixed lateral boundary condition under a mechanical load [26] on the top surface is considered; in the P-FGM case, a different three-layered MEE plate is studied with a simply-supported lateral boundary condition, with applied uniform mechanical traction and electric potential on the top surface. In both cases, the influence of the material grading on the elastic, electric and magnetic responses are discussed.

2. BASIC EQUATIONS AND GENERAL FEM FORMULATION

A general constitutive equation for the magneto-electro-elastic three-phase coupled material can be expressed as

$$\bar{\sigma} = \bar{D}\bar{\gamma} \tag{1}$$

where,

$$\bar{\sigma} = (\,\sigma\ D\ B\,)^T \tag{2}$$

$$\bar{\gamma} = (\,\gamma\ -E\ -H)^T \tag{3}$$

$$\bar{D} = \begin{bmatrix} C & e & q \\ e^T & -\varepsilon & -\alpha \\ q^T & -\alpha^T & -\mu \end{bmatrix} \tag{4}$$

are the extended stress, strain and stiffness vectors (matrices) and a superscript T means the transpose of vector (matrix). In these expressions, σ, D and B are vectors of the elastic stress, electric induction and magnetic displacement; γ, E and H are vectors of the elastic strain, electric field and magnetic field. C, ε, μ, e, q and α are matrices of the elastic stiffness, permittivity, permeability, piezoelectric, piezomagnetic and magnetoelectric coefficients. For a layered multiferroic composite where each layer is either piezoelectric or piezomagnetic material, the extended stiffness matrix (4) is reduced to

$$\bar{D}_{PE} = \begin{bmatrix} C & e & 0 \\ e^T & -\varepsilon & 0 \\ 0 & 0 & -\mu \end{bmatrix} \tag{5}$$

$$\bar{D}_{PM} = \begin{bmatrix} C & 0 & q \\ 0 & -\varepsilon & 0 \\ q^T & 0 & -\mu \end{bmatrix} \tag{6}$$

for the PE and PM layer, respectively.

For a solid brick element with 8 nodes and 5 degrees of freedom (DOFs) on each node, the general strain-displacement equation can be expressed as

$$\bar{\gamma} = \bar{B}\bar{u} \tag{7}$$

$$\bar{u} = (u_1\ \ v_1\ \ w_1\ \ \phi_1\ \ \psi_1\ \ \cdots\ \ u_8\ \ v_8\ \ w_8\ \ \phi_8\ \ \psi_8)^T \tag{8}$$

$$\bar{B} = [B_1\ \ B_2\ \ B_3\ \ B_4\ \ B_5\ \ B_6\ \ B_7\ \ B_8] \tag{9}$$

where $\bar{u}$ is a 40×1 general nodal displacement vector, and each submatrix in $\bar{B}$ can be expressed as

$$B_i = \begin{bmatrix} \frac{\partial N_i}{\partial x} & 0 & 0 & 0 & \frac{\partial N_i}{\partial z} & \frac{\partial N_i}{\partial y} & 0 & 0 & 0 & 0 & 0 & 0 \\ 0 & \frac{\partial N_i}{\partial y} & 0 & \frac{\partial N_i}{\partial z} & 0 & \frac{\partial N_i}{\partial x} & 0 & 0 & 0 & 0 & 0 & 0 \\ 0 & 0 & \frac{\partial N_i}{\partial z} & \frac{\partial N_i}{\partial y} & \frac{\partial N_i}{\partial x} & 0 & 0 & 0 & 0 & 0 & 0 & 0 \\ 0 & 0 & 0 & 0 & 0 & 0 & \frac{\partial N_i}{\partial x} & \frac{\partial N_i}{\partial y} & \frac{\partial N_i}{\partial z} & 0 & 0 & 0 \\ 0 & 0 & 0 & 0 & 0 & 0 & 0 & 0 & 0 & \frac{\partial N_i}{\partial x} & \frac{\partial N_i}{\partial y} & \frac{\partial N_i}{\partial z} \end{bmatrix}^T \tag{10}$$

In Eq. (10), N is the shape function and is evaluated in the intrinsic coordinate:

$$N_i = (1 + \xi\xi_i)(1 + \eta\eta_i)(1 + \zeta\zeta_i)/8, \qquad i = 1, \ldots, 8 \tag{11}$$

where (ξ, η, ζ) denotes the intrinsic coordinate of an arbitrary point and (ξ_i, η_i, ζ_i) the intrinsic coordinate of the ith node in the element.

The Jacobian matrix is defined as:

$$J = \begin{bmatrix} \frac{\partial x}{\partial \xi} & \frac{\partial y}{\partial \xi} & \frac{\partial z}{\partial \xi} \\ \frac{\partial x}{\partial \eta} & \frac{\partial y}{\partial \eta} & \frac{\partial z}{\partial \eta} \\ \frac{\partial x}{\partial \zeta} & \frac{\partial y}{\partial \zeta} & \frac{\partial z}{\partial \zeta} \end{bmatrix} \equiv N_d X_n \tag{12}$$

where,

$$N_d = \begin{bmatrix} \frac{\partial N_1}{\partial \xi} & \cdots & \frac{\partial N_8}{\partial \xi} \\ \frac{\partial N_1}{\partial \eta} & \cdots & \frac{\partial N_8}{\partial \eta} \\ \frac{\partial N_1}{\partial \zeta} & \cdots & \frac{\partial N_8}{\partial \zeta} \end{bmatrix} \tag{13}$$

$$X_n = \begin{bmatrix} x_1 & y_1 & z_1 \\ \vdots & \vdots & \vdots \\ x_8 & y_8 & z_8 \end{bmatrix} \tag{14}$$

with (x_i, y_i, z_i) $(i = 1, \ldots, 8)$ denoting the global coordinates of node i in the considered element.

The derivatives of the shape functions with respect to the global coordinates can be expressed in terms of those with respect to the intrinsic coordinates:

$$\begin{Bmatrix} \frac{\partial N_i}{\partial x} \\ \frac{\partial N_i}{\partial y} \\ \frac{\partial N_i}{\partial z} \end{Bmatrix} = J^{-1} \begin{Bmatrix} \frac{\partial N_i}{\partial \xi} \\ \frac{\partial N_i}{\partial \eta} \\ \frac{\partial N_i}{\partial \zeta} \end{Bmatrix} \qquad (i = 1, \ldots, 8) \tag{15}$$

Considering the principle of virtual work

$$\int_V \bar{\sigma}^T \delta \bar{\gamma} dv = \delta \bar{u}^T F_e \tag{16}$$

in terms of the discretized extended nodal force and displacement vectors, we finally arrived at the following linear algebraic equation between the extended nodal force vector F_e and displacement vector $\bar{u}$.

$$F_e = K_e \bar{u} \tag{17}$$

where K_e is the extended element stiffness matrix in the discretized system, i.e.,

$$K_e = \int_V \bar{B}^T \bar{D} \bar{B} dv \tag{18}$$

which can be calculated by the Gauss integration:

$$\int_V B^T(x, y, z) D(x, y, z) B(x, y, z) dx dy dz = \int_{-1}^{1} \int_{-1}^{1} \int_{-1}^{1} \times B^T(\xi, \eta, \zeta) D(\xi, \eta, \zeta) B(\xi, \eta, \zeta) |J| \, d\xi d\eta d\zeta \tag{19}$$

where $|J|$ is the determination of the Jacobian matrix. It should be pointed out that the material stiffness matrix D in Eq. (19) is not a constant for FGM structures as discussed below.

3. GRADED MATERIAL PROPERTIES

There are mainly three types of functions defining the variation of material properties in the previous research: an exponential function called **E-FGM** [23, 26 and 28], a power-law function called **P-FGM** [29–31], and a sigmoid function composed of two power-law functions called S-FGM [32–34]. While all these grading variations can be easily included in our 3D FEM program, in this article, we focus on the E-FGM and P-FGM cases.

3.1. E-FGM

The E-FGM stiffness matrix can be constructed similar to that in [26]:

$$\mathbf{D} = \mathbf{D_1} e^{k z_r} \tag{20}$$

where $\mathbf{D_1}$ is the stiffness matrix at the top or bottom surface of the layer and k is the exponential coefficient; z_r is the relative height along the thickness of the layer and has a value between 0 and 1; $e^{k z_r}$ is called the proportional factor of the material stiffness matrix. Figure 1 shows the proportional factors for different k values, varying along the thickness direction of a three-layered MEE composite. The top and bottom layers are both piezomagnetic E-FGM with symmetric proportional factor and the middle layer is homogenous piezoelectric with stiffness matrix $\mathbf{D_E}$. For this special layered composite, the exponential grading function is defined in the top layer as:

$$\mathbf{D} = \mathbf{D_M} e^{k z_r} \tag{21}$$

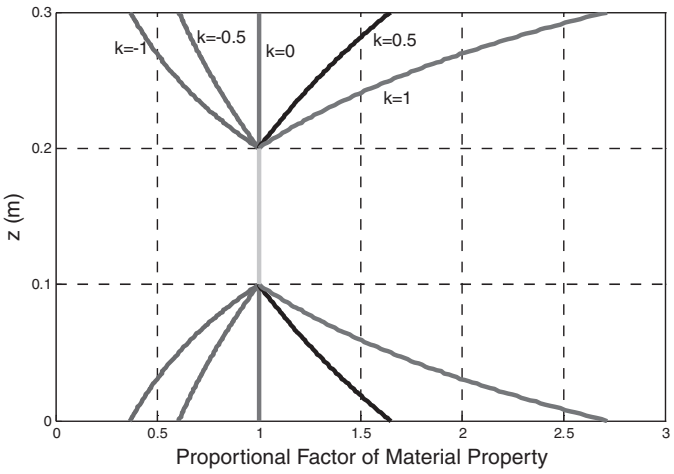

FIG. 1. Variation of the material proportional factor along the thickness direction for a three-layered E-FGM composite. For $z \in$[0.2,0.3 m], the coefficient is calculated using $e^{10k(z-0.2)}$ with $k = -1, -0.5, 0, 0.5, 1$ and for $z \in$[0,0.1m] it is obtained by symmetric requirement.

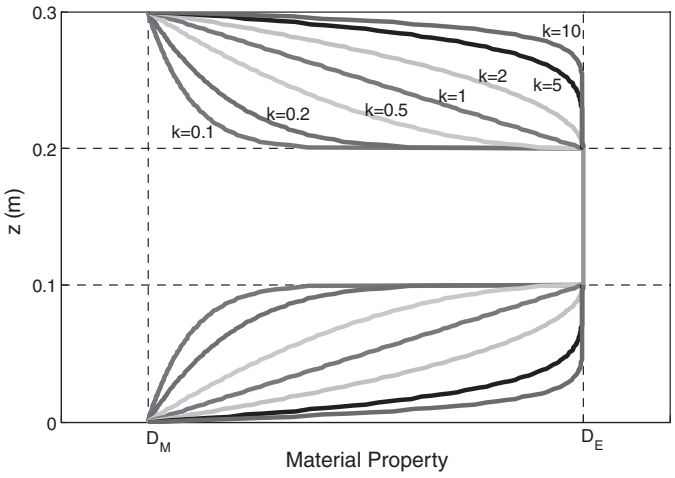

FIG. 2. Variation of the material property along the thickness direction for a three-layered P-FGM composite. For $z \in$[0.2,0.3 m], the material property is calculated by $D = (1-(10(z-0.2))^k)D_M + (10(z-0.2))^k D_E$ with $k = 0.1$, 0.2, 0.5, 1, 2, 5, 10 and for $z \in$[0,0.1m] it is obtained by symmetric requirement.

Note that the material stiffness at the interface is not continuous and $k = 0$ corresponds to the three-layered case with all of them being homogenous, that is, the FBF case in [8].

3.2. P-FGM

A power-law function:

$$\mathbf{D} = \left(1 - z_r^k\right)\mathbf{D_1} + z_r^k\mathbf{D_2} \tag{22}$$

is used to define the graded material property for P-FGM composite. In Eq. (22), $\mathbf{D_1}$ and $\mathbf{D_2}$ denote the material stiffness matrices at the top and bottom surfaces of the layer, respectively, and $\mathbf{D}$ is, therefore, the effective stiffness matrix in the layer, which obviously varies continuously along the thickness direction. Figure 2 shows the variation of the material stiffness matrix for different k, varying along the thickness direction of the three-layered MEE composite. The top and bottom layers are P-FGM with symmetric material properties, and the middle layer is homogenous piezoelectric material with stiffness matrix $\mathbf{D_E}$. The power-law grading function for this specific case is defined as:

$$\mathbf{D} = \left(1 - z_r^k\right)\mathbf{D_E} + z_r^k\mathbf{D_M} \tag{23}$$

in the top layer. It is observed from Figure 2, although the material property is continuous at the interfaces of the layers, different power coefficients k correspond to different degrees of material property variation. It is noticed that while $k = 0.1$ corresponds to a sharp change in the material property at interface, $k = 1$ corresponds to a linearly graded material.

In the numerical integration for calculating the element stiffness matrix, the graded material property needs to be computed. Different from the approximate method in [24], in this article, the coordinates of the Gauss points are directly substituted into the material property functions and thus an exact material stiffness is obtained at the Gauss points, avoiding the error from the approximate shape functions.

4. NUMERICAL EXAMPLES

The three-layered composites (Figure 3) with E-FGM and P-FGM grading layers are solved in this section. To precisely capture the field distribution along the thickness direction, the mesh density in the z-direction is set finer than those in the in-plane directions, i.e., a mesh grid $n_x \times n_y \times n_z = 10 \times 10 \times 30$ is used.

We consider, first, an E-FGM three-layered multiferroic composite model (Figure 3a) similar to the one in [26]. The top and bottom layers are piezomagnetic E-FGM material $CoFe_2O_3$ and the middle layer is homogenous piezoelectric material $BaTiO_3$. The proportional factors of the material stiffness in Figure 1 are adopted. Material properties of $CoFe_2O_3$ and $BaTiO_3$ are list in Table 1. Note that for the piezomagnetic material $CoFe_2O_3$, the permeability coefficients along the x- and y-directions are taken to be positive rather than negative [8, 26]. The layered plate has the geometric dimensions $L_x = L_y = 1$m and $t_1 = t_2 = t_3 = 0.1$m. A mechanical load

$$\sigma_{zz} = \sin\frac{\pi x}{L_x}\sin\frac{\pi y}{L_y} \qquad (N/m^2) \tag{24}$$

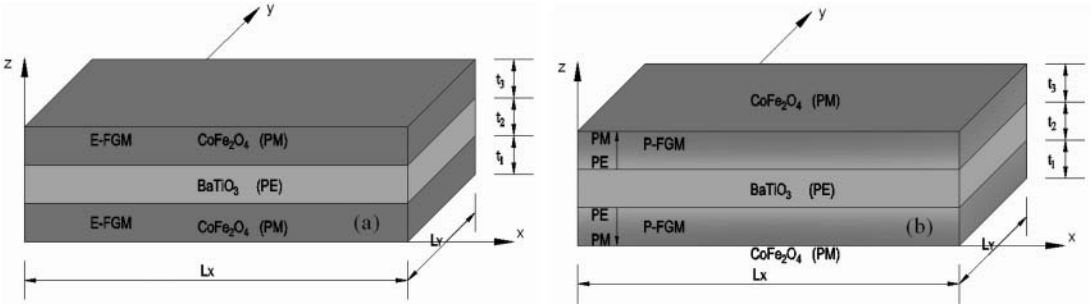

FIG. 3. Three-layered FGM multiferroic composites with a homogenous piezoelectric material in the middle: Top and bottom layers are single phase piezomagnetic with grading E-FGM in (a); top and bottom layers are PE/PM with grading P-FGM in (b).

TABLE 1
Material properties of $BaTiO_3$ and $CoFe_2O_4$ [8, 26](C_{ij}: elastic constants in GPa; e_{ij}: piezoelectric coefficients in N/(Vm); q_{ij}: piezomagnetic coefficients in N/(Am); ε_{ij}: permittivity coefficients in 10^{-9} C/(Vm); and μ_{ij}: permeability coefficients in 10^{-6} Wb/(Am)

	$BaTiO_3$	$CoFe_2O_4$		$BaTiO_3$	$CoFe_2O_4$
C_{11}	166	286	q_{13}	0	580.3
C_{12}	77	173	q_{23}	0	580.3
C_{13}	78	170.5	q_{33}	0	699.7
C_{22}	166	286	q_{42}	0	550
C_{23}	78	170.5	q_{51}	0	550
C_{33}	162	269.5	ε_{11}	11.2	0.08
C_{44}	43	45.3	ε_{22}	11.2	0.08
C_{55}	43	45.3	ε_{33}	12.6	0.093
C_{66}	44.5	56.5	μ_{11}	5	590
e_{13}	−4.4	0	μ_{22}	5	590
e_{23}	−4.4	0	μ_{33}	10	157
e_{33}	18.6	0			
e_{42}	11.6	0			
e_{51}	11.6	0			

is applied on the top surface while all other extended traction components are zero. On the bottom surface, it is traction free (i.e., $\sigma_{xz} = \sigma_{yz} = \sigma_{zz} = D_z = B_z = 0$). For the simply supported lateral boundary condition case, we found that our 3D FEM results coincide very well with the exact solutions in [26] (using exactly the same material properties as in [26]). For instance, Table 2 compares the elastic displacements, electric and magnetic potentials based on the present 3D FEM with those from the exact solutions [26] at field point

TABLE 2
Comparison of the elastic displacements (10^{-14} m), electric potential (10^{-3} V) and magnetic potential (10^{-7} A) between the present 3D FEM solution and the exact one by Pan and Han [26] for the E-FGM three-layered multiferroic composite. A mechanical load is applied on the top surface while the lateral boundaries are simply supported [26]. The exponential coefficient of the E-FGM is k = 0 and 1, and the field point is at (x,y,z) = (0.8 m,0.2 m,0.2 m).

	k = 0		k = 1	
	Present FEM	Exact solution [26]	Present FEM	Exact solution [26]
u_x	27.13	27.47	6.887	7.181
u_y	−27.13	−27.47	−6.887	−7.181
u_z	346.8	345.3	225.2	223.8
ϕ	1.651	1.619	1.514	1.490
ψ	−13.66	−13.29	−8.362	−8.133

(x,y,z) = (0.8m,0.2m,0.2m). It is obvious that using even a coarse mesh grid $n_x \times n_y \times n_z = 10 \times 10 \times 30$, the relative error from the present 3D FEM is only about 4%.

Now we assume a fixed lateral boundary condition to the layered plate (i.e., the extended displacement vector is zero) and calculate the field variation in the z-direction at the fixed horizontal coordinate ($x = 0.75$m, $y = 0.25$m). Figures 4a–4h show, respectively, the variations of the electric potential ϕ in Volt (V), magnetic potential ψ in Ampere (A), elastic stress σ_{xx} in N/m^2, elastic stress σ_{zz}, electric displacement D_x in Coulomb/m^2 (C/m^2), electric displacement D_z, magnetic induction B_x in Weber/m^2 (Wb/m^2) and magnetic induction B_z along the thickness direction of the composite (from z = 0 to z = 0.3m). It is observed that: 1). Because of the material mismatch, the field variation (except for σ_{zz}) shows clearly either a discontinuity (σ_{xx}, D_x, and B_x) or slope discontinuity (ϕ, ψ, D_z, and B_z) at the two interfaces of the composite; 2). Material grading has obvious effects on both the electric and magnetic potentials in all the three layers (even in the middle homogeneous layer, Figures 4a and 4b), on D_x in the middle layer (Figure 4e), and on other field quantities (except for σ_{zz}) in both the top and bottom layers (Figures 4c, 4f, 4g, and 4h).

The second example is a P-FGM three-layered MEE composite (Figure 3b) with material variation shown in Figure 2. The top and bottom layers are PE/PM with grading P-FGM and the middle layer is a homogenous PE material. The lateral boundary condition of the layered plate is assumed to be simply supported. On the top and bottom surfaces, two boundary condition cases are considered: In the first case, a uniform mechanical traction

$$\sigma_{zz} = -1 \qquad (N/m^2) \tag{25}$$

is applied to the top surface, while the other extended traction components are zero. On the bottom surface, it is traction free. In the second case, a uniform electric potential

$$\phi = 1 \qquad (V) \tag{26}$$

is applied on the top surface, whilst the elastic traction and B_z are zero. Similarly, on the bottom surface, it is traction free.

Figure 5 shows the field variation induced by the mechanical load (Eq. (25)) at the fixed horizontal coordinate ($x = 0.75$ m, $y = 0.25$ m) along the thickness direction of the composite (from $z = 0$ to $z = 0.3$ m). It is observed that, different to the exponential grading case (Figures 4c, 4d), the horizontal and vertical normal stresses (Figures 5c, 5d) are nearly independent of power coefficient k. In other words, the k value has a greater influence on the electric displacement and magnetic induction than on the elastic stresses. Furthermore, it is noticed that: 1). For both the electric and magnetic potentials, a larger k corresponds to a smaller magnitude of them (Figures 5a, 5b); 2). With

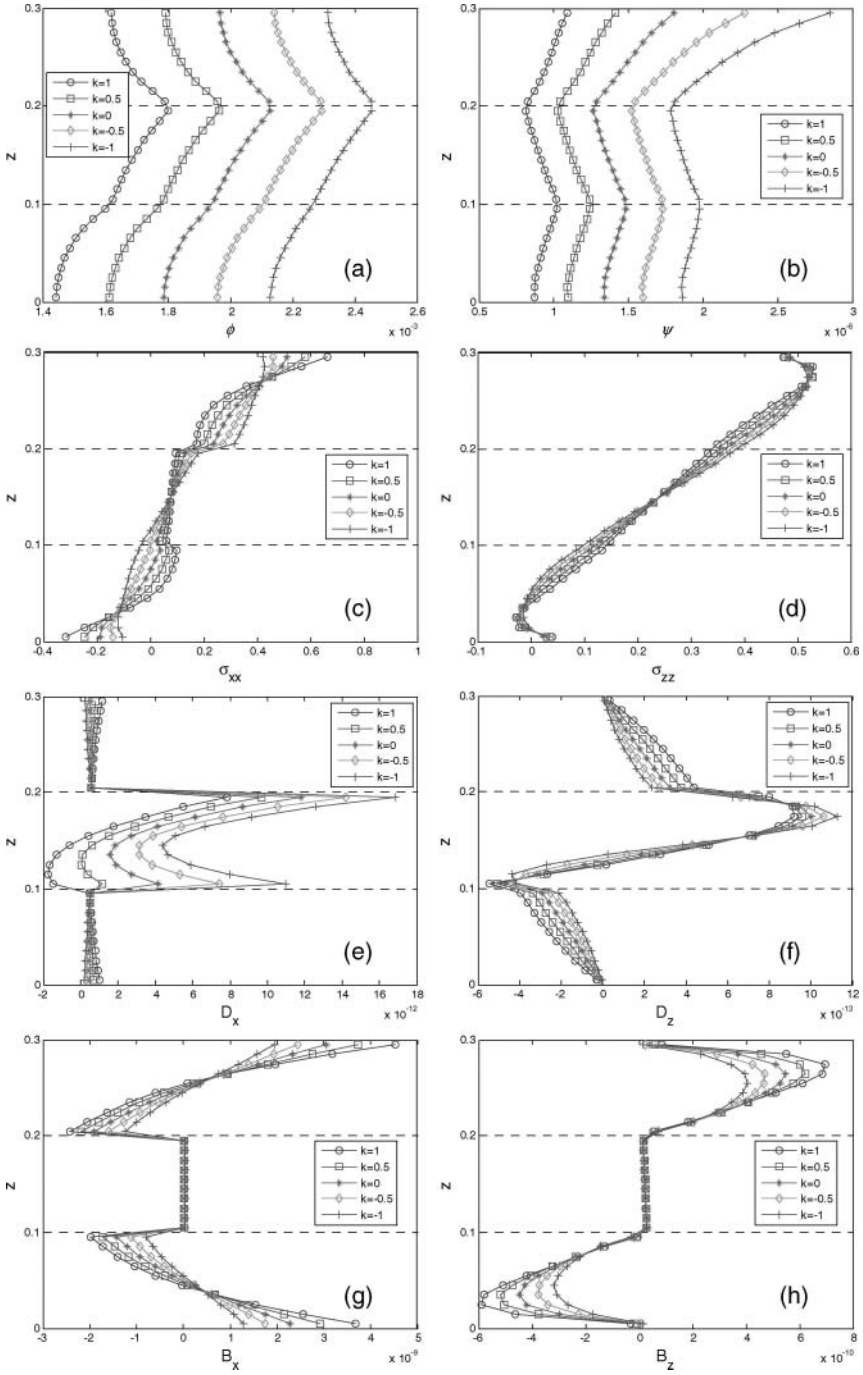

FIG. 4. Variation of the electric potential in (a) (in V), magnetic potential in (b) (in A), elastic stresses in (c) and (d) (in N/m^2), electric displacements in (e) and (f) (in C/m^2) and magnetic inductions in (g) and (h) (in Wb/m^2) along the thickness direction in the three-layered E-FGM multiferroic composite with fixed lateral boundary condition induced by a mechanical load on the top surface.

increasing power coefficient k, the field quantities become smoother, which is consistent with the grading variation in Figure 2, where a small k corresponds to a sharp change of material properties at interfaces; 3). A large value of k results in a large electric displacement (Figure 5e, 5f) as this corresponds to a large volume ratio of piezoelectric phase in the FGM layer. Similarly, a small value of k results in a large magnetic induction (Figure 5g, 5h) due to the large volume ratio of piezomagnetic phase in the FGM layer; 4). Because the piezomagnetic coefficients of the piezoelectric material $BaTiO_3$ are zeros, for any

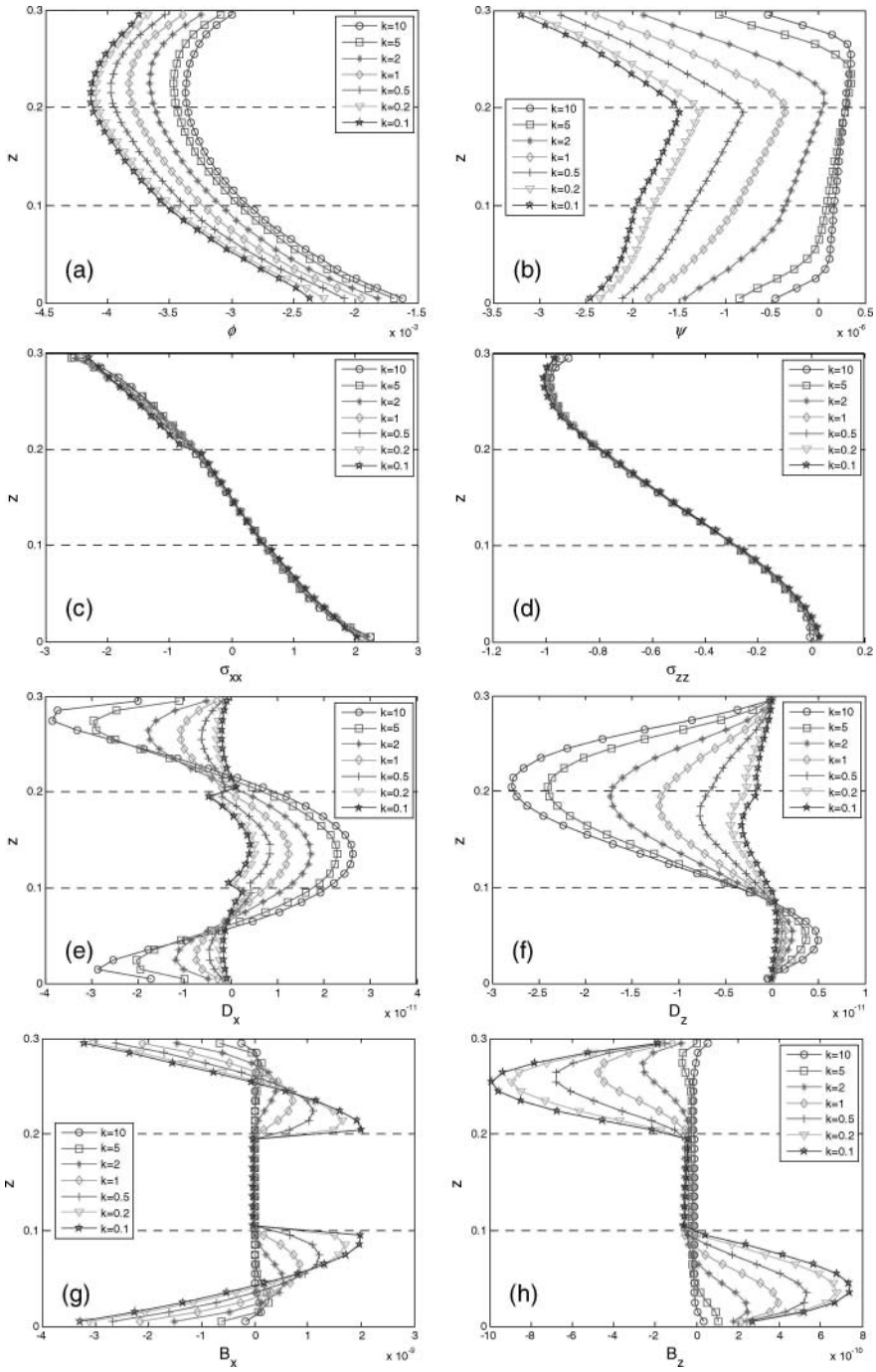

FIG. 5. Variation of the electric potential in (a) (in V), magnetic potential in (b) (in A), elastic stresses in (c) and (d) (in N/m^2), electric displacements in (e) and (f) (in C/m^2) and magnetic inductions in (g) and (h) (in Wb/m^2) along the thickness direction in the three-layered P-FGM multiferroic composite with simply-supported lateral boundary condition induced by a mechanical load on the top surface.

value of k, the magnetic induction in the homogenous piezoelectric layer (middle) is close to zero (Figures 5g, 5h).

Figure 6 shows the field variation induced by the electric load (Eq. (26)) at the fixed horizontal coordinate ($x = 0.75$ m, $y = 0.25$ m) along the thickness direction of the composite (from $z = 0$ to $z = 0.3$ m). It is observed that: 1). A large value of k corresponds to a large magnitude of the electric and magnetic potentials; 2). As compared to the mechanical load case (Figures 4c, 4d, Figures 5c, 5d), the stresses (Figures 6c and 6d) are more sensitive to the power coefficient k. In general, a large k corresponds to a large magnitude of the stresses; 3). As k increases from 0.1 to 10, the magnitude of both electric

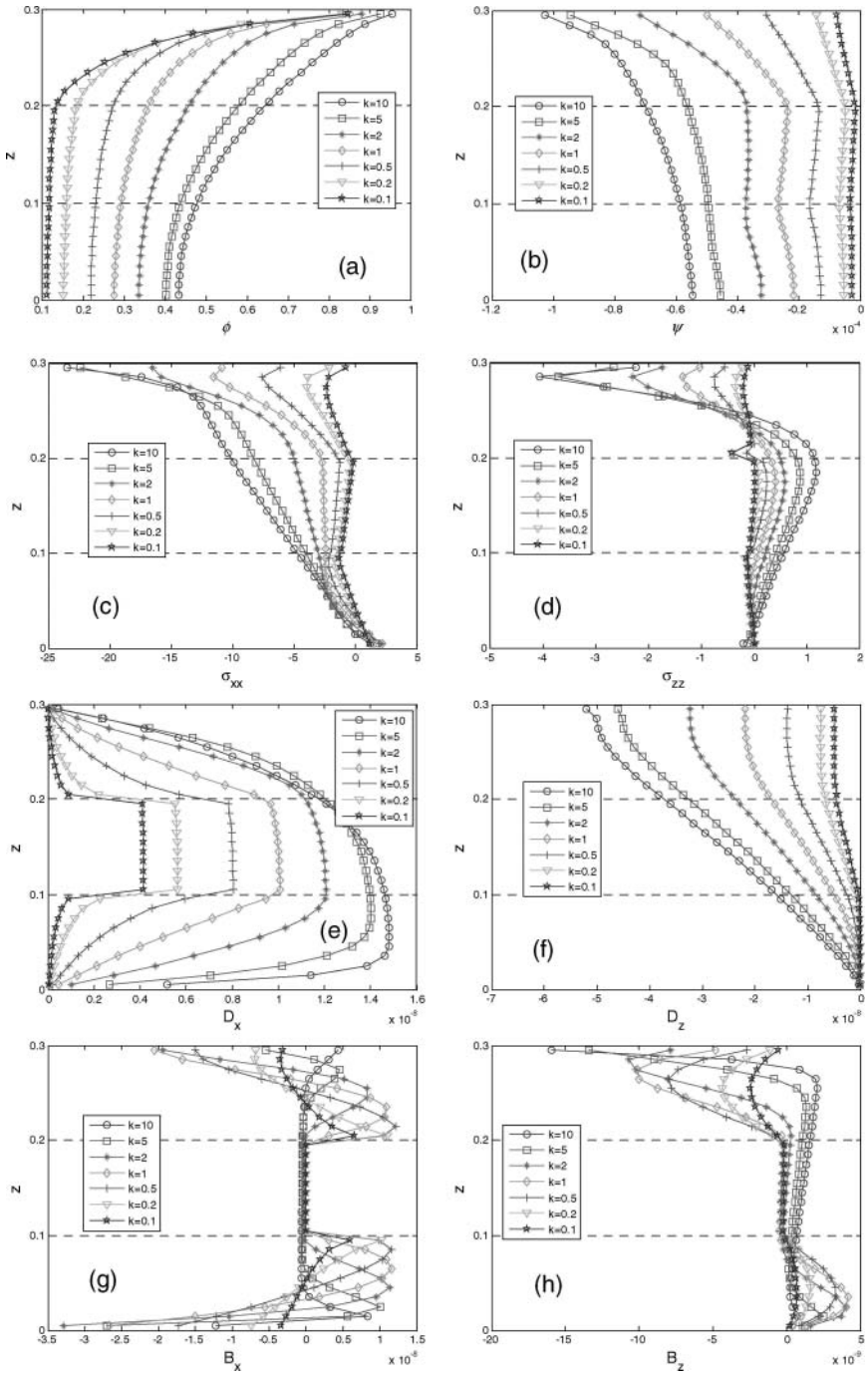

FIG. 6. Variation of the electric potential in (a) (in V), magnetic potential in (b) (in A), elastic stresses in (c) and (d) (in N/m^2), electric displacements in (e) and (f) (in C/m^2) and magnetic inductions in (g) and (h) (in Wb/m^2) along the thickness direction in the three-layered P-FGM multiferroic composite with simply-supported lateral boundary condition induced by an electric potential on the top surface.

displacements increases (Figure 6e, 6f); 4). For large k, the normal stress σ_{zz} (Figure 6d) and normal magnetic induction B_z (Figure 6h) on the top and bottom surfaces are different from zero. This is due to the factor that a large k corresponds to a steep material property gradient near the surface, as can be clearly observed from Figure 2. Therefore, a dense mesh in the vertical direction would be required near the surface in order to obtain more accurate results on the field response.

5. CONCLUSIONS

A 3D FEM program is developed for FGM multiferroic composite analysis. The formulation is based on the 8-node brick

elements with integration of the material stiffness for any given grading material. Both the exponential and power-law functions are assumed in the top and bottom layers of the three-layered composites (with the middle layer being homogeneous) and the following conclusions can be drawn from our FEM modeling:

1. Different grading functions correspond to different field responses, and due to the material mismatch, the field response along the thickness direction of the layered plate is either discontinuous or has a discontinuous slope across the interface.
2. Under a mechanical load, the electric displacements and magnetic inductions are more sensitive than the stresses to the material grading; under an electric load, on the other hand, material grading affects all field responses.
3. For the mechanical load case, a grading coefficient k which produces a large volume ratio of the piezoelectric (piezomagnetic) phase in the layered plate would result in a large magnitude of the piezoelectric displacement (magnetic induction) response.
4. The electric displacement (magnetic induction) responses are relatively smaller in the purely piezomagnetic (piezoelectric) material layer as compared to these in the adjacent layer.

ACKNOWLEDGEMENTS

This work was partially supported by AFOSR FA9550-06-1-0317. We also thank the reviewers for their helpful comments.

REFERENCES

1. C.W. Nan, Magnetoelectric Effect in Composites of Piezoelectric and Piezomagnetic. Phases, Phys. Rev. B, vol. 50, pp. 6082–6088, 1994.
2. M.I. Bichurin, V.M. Petrov, and G. Srinivasan, Theory of Low-frequency Magnetoelectric Effects in Ferromagnetic-ferroelectric Layered Composites, J. Appl. Phys., vol. 92, pp. 7681–7683, 2002.
3. M.I. Bichurin, V.M. Petrov, and G. Srinivasan, Theory of Low-frequency Magnetoelectric Coupling in Magnetostrictive-piezoelectric Bilayers, Phys. Rev. B, vol. 68, 054402-1-13, 2003.
4. S. Dong, J.F. Li, and D. Viehland, Longitudinal and Transverse Magnetoelectric Voltage Coefficients of Magnetostrictive/piezoelectric Laminate Composite: Theory, IEEE Trans. Ultrason. Ferroelectr. Freq. Control, vol 50, 1253–1261, 2003.
5. S. Dong, J. Zhai, J.F. Li, et al., Magnetoelectric Gyration Effect in $Tb_{1-x}Dy_xFe_{2-y}$/Pb(Zr,Ti)O_3 Laminated Composites at The Electromechanical Resonance, Appl. Phys. Lett, vol 89, 243512-1-3, 2006.
6. V.M. Petrov and G. Srinivasan, Enhancement of Magnetoelectric Coupling in Functionally Graded Ferroelectric and Ferromagnetic Bilayers, Phys. Rev. B, vol. 78, 184421-1-8, 2008.
7. M. Fiebig, Revival of The Magnetoelectric Effect, Topical Review, J. Phys. D, vol. 38, pp. R123–152, 2005.
8. E. Pan, Exact Solution for Simply Supported and Multilayered Magneto-electro-elastic Plates, J. Appl. Mech., vol. 68, 608–618, 2001.
9. E. Pan and P.R. Heyliger, Free Vibrations of Simply Supported and Multilayered Magneto-electro-elastic Plates, J. Sound. Vib., vol. 252, 429–442, 2002.
10. E. Pan and P.R. Heyliger, Exact Solutions for Magneto-electro-elastic Laminates in Cylindrical Bending, Int. J. Solids Struct., vol. 40, pp. 6859–6876, 2003.
11. R.G. Lage, C.M.M. Soares, C.A.M. Soares, et al., Layerwise Partial Mixed Finite Element Analysis of Magneto-electro-elastic Plates, Comput. Struct., vol. 82, pp. 1293–1301, 2004.
12. R.K. Bhangale and N. Ganesan, Static Analysis of Simply Supported Functionally Graded And Layered Magneto-Electro-Elastic Plates, Int. J. Solids Struct., vol. 43, pp. 3230–3253, 2006.
13. M. Niino, T. Hirai, and R. Watanabe, The Functionally Gradient Materials, Jpn. Soc. Comp. Mat, vol. 13, pp. 699, 1987.
14. K. Ichikawa, Functionally Graded Materials in 21st Century, pp. 18–20, Springer, New York, 2000.
15. Y.S. Wang, G.Y. Huang, and D. Dross, On The Mechanical Modeling of Functionally Graded Interfacial Zone with A Griffith Crack: Anti-plane Deformation, J. Appl. Mech, vol. 70, pp. 676–680, 2003.
16. G.Y. Huang, Y.S. Wang, and S.W. Yu, Fracture Analysis of A Functionally Graded Interfacial Zone under Plane Deformation, Int. J. Sol. Struct., vol. 41, pp. 731–743, 2004.
17. N.T. Hart, N.P. Brandon, M.J. Day, et al., Functionally Graded Composite Cathodes for Solid Oxide Fuel Cells, J. Power Sources, vol. 106, pp. 42–50, 2002.
18. S. Zha, Y. Zhang, and M. Liu, Functionally Graded Cathodes Fabricated by Sol-gel/slurry Coating for Honeycomb SOFCs, Solid State Ionics, vol. 176, pp. 25–31, 2005.
19. W. Pompe, H. Worch, M. Epple, et al., Functionally Graded Materials for Biomedical Applications, Mat. Sci. Eng., vol. A362, pp. 40–60, 2003.
20. Y. Yamasaki, Y. Yoshida, M. Okazaki, et al., Synthesis of Functionally Graded $MgCOD_3$ Apatite Accelerating Osteoblast Adhesion, J. Biomed. Mater. Res. A, vol. 62, pp. 99–105, 2002.
21. D. Menon, J. Sargentoni, S. Taylor-Robinson, et al., Effect of Functional Grade and Etiology on In Vivo Hepatic Phosphorus-31 Magnetic Resonance Spectroscopy in Cirrhosis: Biochemical Basis of Spectral Appearances, Hepatology, vol. 21, pp. 417–427, 2005.
22. E. Pan, Exact Solution for Functionally Graded Anisotropic Elastic Composite Laminates, J. Compos. Mater., vol. 37, pp. 1903–1920, 2003.
23. F. Han, E. Pan, A.K. Roy, et al., Response of Piezoelectric, Transversely Isotropic, Functionally Graded, and Multilayered Half Space to Uniform Circular Surface Loadings, CMES-Comp. Model. Eng., vol. 14, pp. 15–29, 2006.
24. J.H. Kim and G.H. Paulino, Isoparametric Graded Finite Elements for Nonhomogeneous Isotropic and Orthotropic Materials, J. Appl. Mech., vol. 69, pp. 502–514, 2002.
25. J.H. Kim and G.H. Paulino, Finite Element Evaluation of Mixed Mode Stress Intensity Factors in Functionally Graded Materials, Int. J. Numer. Meth. Eng., vol. 53, pp. 1903–1935, 2002.
26. E. Pan and F. Han, Exact Solution for Functionally Graded and Layered Magneto-electro-elastic Plates, Int. J. Eng. Sci., vol. 43, pp. 321–339, 2005.
27. F. Ramirez, P.R. Heyliger and E. Pan, Discrete Layer Solution to Free Vibrations of Functionally Graded Magneto-electro-elastic Plates, Mech. Adv. Mater. Struc., vol. 13, pp. 249–266, 2006.
28. N. Tutuncu, Stresses in Thick-walled FGM Cylinders with Exponential-varying Properties, Eng. Struct., vol. 29, pp. 2032–2035, 2007.
29. G. Bao and L. Wang, Multiple Cracking in Functionally Graded Ceramic/Metal Coatings, Int. J. Solids. Struct., vol. 32, pp. 2863–2871, 1995.
30. Y.D. Lee and F. Erdogan, Residual/thermal Stresses in FGM and Laminated Thermal Barrier Coatings, Int. J. Fracture, vol. 69, pp. 145–165, 1994.
31. Y.A. Kang and X.F. Li, Bending of Functionally Graded Cantilever Beam with Power-law Non-linearity Subjected to an End Force, Int. J. Non-linear. Mech., vol. 44, pp. 696–703, 2009.
32. S.H. Chi and Y.L. Chung, Mechanical Behavior of Functionally Graded Material Plates under Transverse Load-Part I: Analysis, Int. J. Solids. Struct., vol. 43, pp. 3657–3674, 2006.
33. S.H. Chi and Y.L. Chung, Mechanical Behavior of Functionally Graded Material Plates under Transverse Load-Part II: Numerical Results, Int. J. Solids. Struct., vol. 43, pp. 3675–3691, 2006.
34. S. Ben-oumrane, T. Abedlouahed, M. Ismail and B.B. Mohamed, A Theoretical Analysis of Flexional Bending of Al/Al_2O_3 S-FGM Thick Beams, Comp. Mater. Sci., vol. 44, pp. 1344–1350, 2009.